

# NUMERICAL METHOD FOR ANALYZING INTERACTION AND COALESCENCE OF NUMEROUS MICROCRACKS

Xi-Qiao Feng, Lin Ma, and Shou-Wen Yu

*Department of Engineering Mechanics, Tsinghua University, Beijing 100084, China*

*Email: Fengxq@tsinghua.edu.cn; Yusw@tsinghua.edu.cn*

## ABSTRACT

In this paper, a numerical method is presented for calculating the effective elastic moduli and the tensile strength as well as for simulating the failure process of brittle materials associated with microcracking damage. By introducing two criteria for microcrack growth and coalescence in terms of Griffith's energy release rate, the above numerical method is used here to simulate the coalescence process of microcracks that results in a fatal crack and the final rupture of a specimen.

## 1 INTRODUCTION

The dependences of mechanical properties (e.g., constitutive relation, strength, toughness and conductivity) of materials on interacting microcracks can be divided into two types, weak (or indirect) and strong (or direct). The micromechanics approaches dealing with these two types of interaction problems are of great difference. Various methods (e.g., self-consistent method, generalized self-consistent method and differential method) have been established for estimating the impacts of microcrack interaction on the effective elastic moduli of microcracked solids [1–4]. These methods, with few exceptions, are based on the concept of effective (equivalent) medium or effective stress field, and omit concrete positions and orientations of individual microcracks. To date, however, estimation of effective elastic moduli of microcracked solids is still a problem of extensive arguments. On one hand, the accuracy and the validation scopes of these established methods are yet to be evaluated further. On the other hand, there is a lack of experimental data available in the literature for effective moduli of microcracked solids, especially for materials with microcracks of high density. For these reasons, it seems a promising approach to calculate the effective moduli for complex distributions and to evaluate the accuracy of these micromechanics schemes via numerical schemes. Nevertheless, little work of direct numerical analysis has been conducted on this subject because of the high complexity in dealing with microcracks of a large number [5–7].

With regard to strong microcrack interaction, some approximate micromechanics schemes (e.g., pseudo-traction method, complex potential method, and double potential method) and finite element methods have been developed to determine the stress intensity factors (SIFs) of multiple interacting microcracks of a specified array. The problem of interaction of multiple microcracks is often reduced to a set of integral equations, which can be solved by series expansion, perturbation, collocation, and some other approximate techniques. However, the number of equations increases very rapidly with the increase in the number of microcracks. Recently, Feng et al. [6] suggested a micromechanics method for calculating direct interaction of microcracks of a large number, as in most actual brittle materials. They carried out systematic examinations of some factors of microcrack distributions on the effective elastic moduli and strengths of brittle solids.

In addition, the failure behaviors of brittle solids are generally preceded by coalescence of interacting microcracks to form a fatal crack that will propagate unstably. Simulation of material failure characterized by microcrack growth and linkage presents an issue of extensive interest both in theoretical analysis and in engineering applications. Due to the inherent prohibitive complexity and difficulties in calculation, nevertheless, little attention has been paid on the stochastic coalescence process of disordered microcracks. In this paper, strong interaction and coalescence of stochastically distributed microcracks are studied using the effective field-subregion model developed recently by Feng et al. [6]. The failure process of brittle specimens resulting from evolution of randomly distributed microcracks is simulated.

## 2 CALCULATION METHOD

### 2.1. Approximate model

Consider a plate containing many randomly distributed, planar microcracks and subjected to a uniform stress  $\sigma_\infty$  in the far field, as shown in Fig. 1(a). Let us consider a microcrack in it, say the  $\alpha$ th one, whose length is denoted as  $2l_\alpha$ . Refer to a global Cartesian coordinate system ( $o-x_1x_2$ ) and a local one ( $o-x'_1x'_2$ ), as shown in Fig. 1(c), where the  $x'_2$ -axis is parallel to the normal  $\mathbf{n}^\alpha$  of this microcrack. The microcrack orientation is then expressible in terms of an angle,  $\theta_\alpha$ , measured from  $x_2$  to  $\mathbf{n}^\alpha$ . Assume that the statistical distribution of orientations and sizes of microcracks satisfies a probability density function,  $p(l, \theta)$ .

Due to the complexity in calculation of the exact SIFs of the  $\alpha$ th crack interacting with all the other microcracks, some simplifications are made to yield an efficient numerical method. On one hand, the local stress field around a microcrack is highly sensitive to the positions, orientations and sizes of its neighboring cracks. In the present approximate model, therefore, a subdomain  $\Omega$  of the specimen is defined around the  $\alpha$ th microcrack, as shown in Fig. 1(b). The size of  $\Omega$  should be much larger than the characteristic size of microcracks (e.g., 10–20 times the average length of microcracks), while the shape of  $\Omega$  may be specified according to the microcrack orientation distribution. A circular shape is generally appropriate for isotropic or weakly anisotropic distributions of microcracks.

Since all microcracks outside the subdomain  $\Omega$  have been “removed”,  $\Omega$  exists in the plate as a weaker “inclusion” with stiffness lower than the pristine matrix. Neglecting all those microcracks outside leads to an incorrect result that the average stress  $\sigma_\Omega$  over  $\Omega$  is different from  $\sigma_\infty$ . According to Eshelby's inclusion theory [8], the stress and strain fields in an elliptical inclusion, embedded in an otherwise homogeneous infinite matrix, are uniform when a constant stress, denoted by  $\sigma_0$ , is applied in the far field. Thus, the average stress  $\sigma_\Omega$  is expressed as [8]

$$\sigma_\Omega = \mathbf{B} : \sigma_0, \quad (1)$$

where the fourth-order tensor  $\mathbf{B} = [\mathbf{I} + \mathbf{P} : (\mathbf{M} - \mathbf{M}_0)]^{-1}$  is the average stress-concentration tensor,  $\mathbf{P} = \mathbf{M}_0^{-1} : (\mathbf{I} - \mathbf{S})$ ,  $\mathbf{I}$  is the fourth-order identity tensor,  $\mathbf{S}$  is the Eshelby tensor,  $\mathbf{M}_0$  and  $\mathbf{M}$  denote the elastic compliance tensors of the matrix and the subdomain  $\Omega$ , respectively.

If all the microcracks both inside and outside the subregion were considered, the average stress  $\sigma_\Omega$  over  $\Omega$  should equal approximately to the far-field stress  $\sigma_\infty$ . In the approximate model in Fig. 1(b), therefore, we replace the far-field stress  $\sigma_\infty$  by  $\sigma_0$  such that  $\sigma_\Omega = \sigma_\infty$ . From Eq. (1), therefore, the modified far-field stress  $\sigma_0$  should be

$$\boldsymbol{\sigma}_0 = \mathbf{B}^{-1} : \boldsymbol{\sigma}_\infty = [\mathbf{I} + \mathbf{P} : (\mathbf{M} - \mathbf{M}_0)] : \boldsymbol{\sigma}_\infty. \quad (2)$$

To determine the stress concentration tensor  $\mathbf{B}$  in Eq. (2), one need to estimate first the effective compliance tensor  $\mathbf{M}$  of the microcracked inclusion  $\Omega$  by using a micromechanics method [4].

In summary, the central idea of the present method is that the microcracks throughout the specimen  $S$  are skillfully divided into two sets, which are treated in different manners in calculation of their contributions to the SIFs of the  $\alpha$ th crack. The interacting microcracks inside  $\Omega$  are introduced directly from a direct micromechanics method (e.g., Kachanov's method [2, 5]) considering their concrete sizes, locations and orientations, while the influence of those cracks outside is reflected merely by modifying the far-field stress. For further discussions of this global/local method, the reader is referred to Ref. [8].

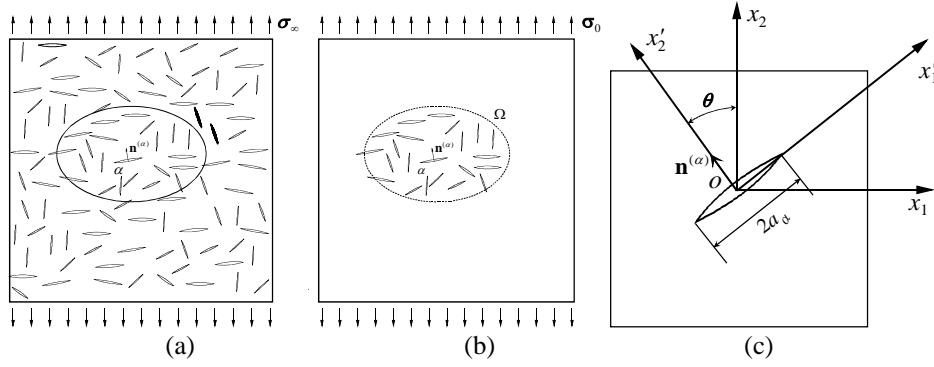


Figure 1. (a) A microcracked solid, (b) the simplified calculation model, and (c) coordinate systems.

## 2.2 Tensile strength

The elastic energy release rate theory developed initially by Griffith is taken here as the controlling indicator of crack growth in brittle solids. Accordingly, the mixed-mode fracture criterion is written as

$$G = (K_I / K_{IC})^2 + (K_{II} / K_{IIC})^2 = 1, \quad (3)$$

where  $K_I$  and  $K_{II}$  denote the mode-I and II SIFs,  $K_{IC}$  and  $K_{IIC}$  their intrinsic critical values, respectively. For simplicity,  $K_{IC}$  and  $K_{IIC}$  are regarded as material constants without dependence upon microcrack propagation. To determine the load-bearing capacity of a specimen, the far-field stress is denoted as  $\boldsymbol{\sigma}_\infty = m\boldsymbol{\sigma}_\infty^0$ , where  $\boldsymbol{\sigma}_\infty^0$  is a tri-axial reference stress tensor, and  $m$  is a load factor. Thus, the  $\alpha$ th crack will undergo an unstable propagation at one of its two tips when the load factor  $m$  reaches the following value

$$m_\alpha = \min \left\{ \left[ \left( \frac{K_{I0}^\alpha(l_\alpha)}{K_{IC}} \right)^2 + \left( \frac{K_{II0}^\alpha(l_\alpha)}{K_{IIC}} \right)^2 \right]^{-1/2}, \left[ \left( \frac{K_{I0}^\alpha(-l_\alpha)}{K_{IC}} \right)^2 + \left( \frac{K_{II0}^\alpha(-l_\alpha)}{K_{IIC}} \right)^2 \right]^{-1/2} \right\}. \quad (4)$$

The tensile strength of a perfectly-brittle specimen is defined as the applied stress  $\boldsymbol{\sigma}_c$  at which any one of the microcracks starts to propagate. That is,

$$\sigma_c = m_c \sigma_\infty^0, \quad (5)$$

where the critical load factor  $m_c$  is the minimum value of  $m_\alpha$  among all the microcracks.

### 3 MICROCRACK COALESCENCE AND FAILURE PROCESS

Failure of a brittle material is often the outcome of a process which involves successive coalescence of interacting microcracks, formation and unstable propagation of a macro crack. In spite of the extensive interest in simulating microcrack coalescence, however, there seems a lack of effective methods for modeling the failure process associated with interaction and evolution of numerous distributed microcracks. To clarify some of the fundamental aspects of the physics of the brittle deformation process we extend our numerical scheme presented above to study coalescence of microcracks and the resulted failure process of microcracked solids.

A key issue for simulating the failure process associated with microcracking is to specify appropriate criteria to determine at each linking step: (i) when microcrack propagation and coalescence will occur, (ii) which microcrack will grow, (iii) with which microcrack it will link, and (iv) the linking path. In fact, difficult is to give a unified criterion for linking of randomly distributed microcracks. The propagation and coalescence path of interacting microcracks are usually curved, even for two collinear cracks. Considering the contradicting requirements of rigor and simplicity, however, we assume that two microcracks are connected always along a straight path and that the linked microcrack, though zigzag, is treated as a planar one in the next coalescing step. These two assumptions was also made by Li and Yang [9], who discussed their acceptable reasonability and accuracy.

Two criteria in terms of the energy release ratio are adopted in our simulation, though other criteria can also be implemented in the present method. First, the SIFs  $K_I$  and  $K_{II}$  and the non-dimensional energy release rates  $G$  of all the microcracks in the considered specimen are calculated in each step by our novel method. The microcrack, denoted as  $A$ , that has the maximum value of  $G$  will propagate in the following step. The critical load for propagation of crack  $A$  is obtained by using the criterion  $G_A=1$  defined in Eq. (3), where the subscript  $A$  stands for a quantity of crack  $A$ .

Besides Eq. (3), another criterion is required to determine which nearby crack will coalesce with  $A$ . For illustration, the right tip of  $A$  in the configuration in Fig. 2(a) may be linked with cracks  $B$ ,  $C$  or  $D$ . The coalescence is dictated here by an energy ratio defined as [9]

$$R = \Delta \Pi / (2c\gamma_s), \quad (6)$$

where  $\Delta \Pi$  denotes the release of potential energy caused by the linking of two neighboring cracks,  $c$  the ligament size, and  $\gamma_s$  the surface energy per unit area of the matrix. The parameter  $R$  represents the ratio between the released potential energy and the energy required to create two surfaces along the broken ligament during the coalescence. The larger the ratio  $R$ , the bigger the driving force of coalescence. Cracks  $A$  and  $B$  will be connected if  $R_{AB}$  is the maximum among  $R_{AI}$ , where  $I$  stands for any of the cracks neighboring to  $A$ .

Then the potential energy contributed from the  $\alpha$  th microcrack can be calculated by

$$\Pi_\alpha = \frac{1}{2} \int_{-l_\alpha}^{l_\alpha} [p^\alpha(\xi) b_2^\alpha(\xi) + \tau^\alpha(\xi) b_1^\alpha(\xi)] d\xi, \quad (7)$$

where  $p^\alpha(\xi)$  and  $\tau^\alpha(\xi)$  denote the normal and shear pseudo-tractions on the surfaces of the  $\alpha$  th crack,  $b_2^\alpha(\xi)$  and  $b_1^\alpha(\xi)$  its opening and sliding displacements [2]. Summing over  $\Pi_\alpha$  before and

after the microcrack linkage, one can obtain the potential energy release  $\Delta \Pi$  and the energy ratio  $R$  from Eq. (6).

In addition, some more complicated situations of microcrack linkage have also been considered in our simulation. An example is schematized in Fig. 2(b). After the crack  $A$  is connected with  $B$ , it is also possible for the right crack tip of  $A$  to coalesce with another crack, say  $C$ , since the SIFs of the connected  $A$ - $B$  crack may be lower than those of  $A$  before connection. The secondary coalescence of the right tip of  $A$ , also governed by the energy ratio, is also accounted for. For similar reasons, it is also possible for a specimen to have several different positions where coalescences occur. This happens mainly in the initial stage of failure.

Before the final rupture of a specimen, there are many coalescence steps. Such a complicated process can be simulated by a step-by-step numerical method. For convenience, only one coalescence is considered in each step of calculation.

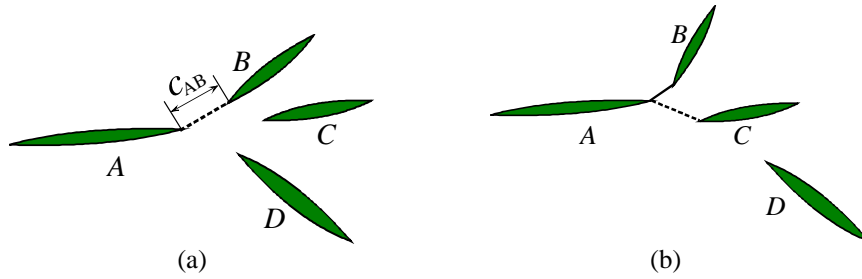


Figure 2. Configurations of microcrack linkage.

#### 4 EXAMPLE

A rectangular concrete specimen of length 0.8m and width 0.4m is taken as an example, which is exposed to uniaxial tension in the  $x_2$  direction. 500 cracks with completely random positions and orientations are produced by a computer program. The crack half-lengths satisfy a normal distribution law  $\Phi(l)$  with the mathematical expectation of 5 mm and the variance of 1 mm. The material parameters are taken as: Young's modulus  $E = 0.35 \times 10^5$  MPa, Poisson's ratio  $\nu = 0.17$ , the critical SIFs  $K_{IC} = 0.165$  MPa  $\cdot$  m<sup>1/2</sup> and  $K_{IIC} = 0.33$  MPa  $\cdot$  m<sup>1/2</sup>. The simulated failure process of such a specimen is given in Fig. 3, which contains 22 steps of linkage before the final rupture. Basically, the zigzag fracture path is normal to the tensile direction. Both the effective modulus and the tensile strength of the specimen have a tendency to decrease during the failure process though some fluctuations exist due to the strong interaction of microcracks and the kinking of the failure path, as shown in Fig. 4. Furthermore, our simulations predict an evident size dependency of failure of brittle materials: a specimen of larger size generally has a lower strength than a smaller specimen with the same microcrack distributions.

#### 5 CONCLUSIONS

An approximate method is presented here to calculate the interaction of microcracks of a large number. Its central idea is that all the microcracks in a specimen are divided into two sets, which are dealt with in different ways. The interacting microcracks within a subdomain around the considered microcrack are calculated by using direct interaction method, while the influence of other microcracks is reflected by modifying the far-field stress.

**Acknowledgements:** The supports from the NSFC and MOE of China are acknowledged.

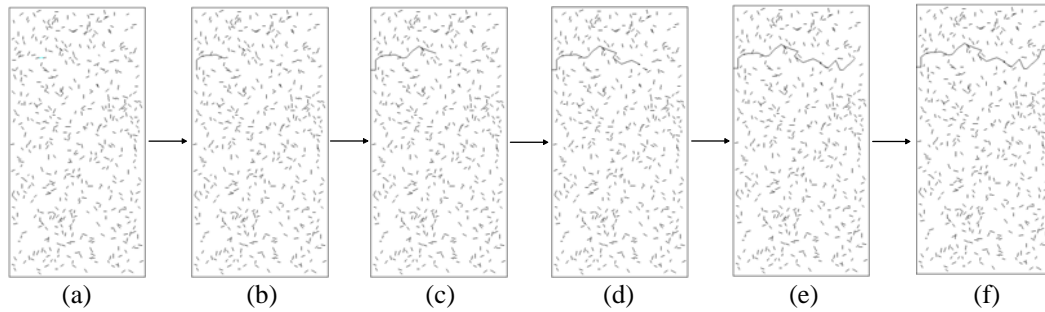


Figure 3. Microcrack coalescence process of a specimen.

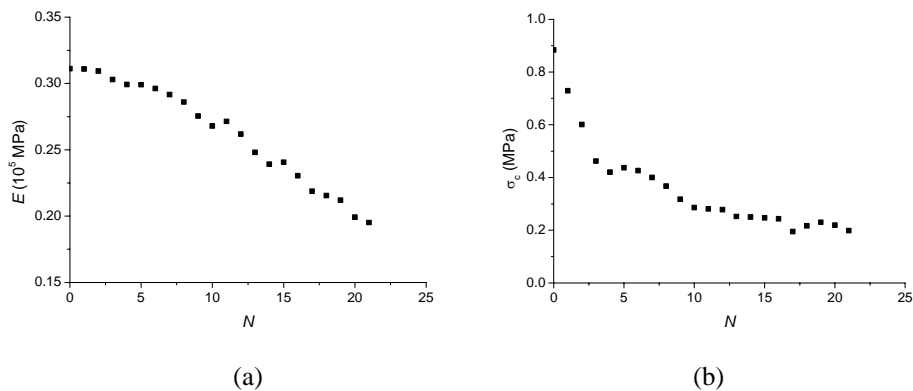


Figure 4. Changes of (a) the Effective Young's modulus and (b) the tensile strength of the specimen during the microcrack coalescence process.

#### REFERENCES

- [1] Krajcinovic, D., *Damage Mechanics*, Amsterdam: Elsevier, 1996.
- [2] Kachanov, M., Elastic solids with many cracks and related problems, *Advances in Applied Mechanics*, 30, 259–445, 1993.
- [3] Yu, S.W., Feng, X.Q., *Damage Mechanics*, Beijing: Tsinghua University Press, 1997.
- [4] Feng, X.Q., Yu, S.W., *Damage Micromechanics of Quasi-Brittle Materials*, Beijing: Higher Education Press, 2002.
- [5] Kachanov, M., Elastic solids with many cracks: A simple method of analysis, *Int. J. Solids. Struct.*, 23, 23–43, 1987.
- [6] Feng, X.Q., Li, J.Y., Yu, S.W., A simple method for calculating interaction of numerous microcracks and applications, *Int. J. Solids. Struct.*, 40, 447–464, 2003.
- [7] Shen, L.X., Li, J., Effective elastic moduli of plates with various distributions and sizes of cracks, *Int. J. Solids. Struct.*, 51, 447–464, 2004.
- [8] Mura, T., *Micromechanics of Defects in Solids*, The Netherlands: Martinus Nijhoff Publishers, 1987.
- [9] Li, T., Yang, W., Critical linkages of coalescing microcracks under stress loading, *Fatigue Fracture Eng. Mater. Struct.*, 25, 499–508, 2002.